

## Generation of Well-directed Flux of THz Radiation in Magnetized Plasma Column Due to Relaxation of Relativistic Electron Beam

A.V. Arzhannikov<sup>1,2</sup>, I.A. Ivanov<sup>1,2</sup>, A.A. Kasatov<sup>1,2</sup>, S.A. Kuznetsov<sup>1,2</sup>, M.A. Makarov<sup>1</sup>,  
K.N. Kuklin<sup>1</sup>, S.S. Popov<sup>1,2</sup>, A.F. Rovenskikh<sup>1</sup>, D.A. Samtsov<sup>1</sup>, E.S. Sandalov<sup>1,2</sup>,  
S.L. Sinitsky<sup>1,2</sup>, V.D. Stepanov<sup>1,2</sup>, V.V. Annenkov<sup>1,2</sup>, V.V. Glinsky<sup>1,2</sup> and I.V. Timofeev<sup>1</sup>

<sup>1</sup>*Budker Institute of Nuclear Physics, Novosibirsk, Russia*

<sup>2</sup>*Novosibirsk State University, Novosibirsk, Russia*

### Introduction

Generation of electromagnetic (EM) radiation due to collective electron beam-plasma interaction is a fundamental phenomenon observed in both cosmic and laboratory plasmas. Such radiation is often the only source of information on wave processes occurring in space plasma [1] or about specific small-scale processes at the plasma confinement in open magnetic trap [2]. In particular, one of the most difficult problems is to explain the mechanisms of cosmic emission of type II and type III solar radio bursts [3].

This problem in many aspects initiated the development of theoretical concepts of plasma turbulence and experiments on the injection of non-relativistic electron beam into a low density ( $<10^{14} \text{ cm}^{-3}$ ) plasma. At these experimental conditions, frequencies of the generated radiation (usually tied to the plasma frequency) were lower than several tens of GHz (for example, see [4]). In experiments at the GOL-PET facility performed at plasma density  $\sim 10^{15} \text{ cm}^{-3}$ , the radiation frequency band is located at several hundred GHz [5]. The aim of these experiments is to generate high-power well-directed flux of THz radiation.

### Experimental set-up

Schematic of the described series of experiments at the GOL-PET facility is presented in Figure 1. The facility consists of the U-2 accelerator producing a high-current REB and an open magnetic trap with a plasma column of varied plasma density. The mean value of the magnetic field is  $B = 4.2 \text{ T}$  and the length of the trap is about  $L = 1.5 \text{ m}$ . A plasma column with a diameter of 6 cm is created in a quartz tube of 8 cm inner diameter installed in a stainless-steel vacuum chamber. The plasma column production is realized in the following way. Pulse gas valves generate a hydrogen cloud with the necessary spatial distribution. A high voltage discharge in gas with the current of about 20 kA generates a plasma column with variable density in the range  $(0.8-3) \cdot 10^{15} \text{ cm}^{-3}$ . The density distribution over the column diameter is measured by a six-channel Thompson scattering system ( $\lambda = 1.053 \text{ }\mu\text{m}$ ). To measure the linear plasma density along the column diameter we use an interferometer at a wavelength 10.6  $\mu\text{m}$ . The power of THz radiation fluxes escaping from the plasma column

both along and perpendicular to its axis was measured after going out to atmosphere through fluoroplastic windows. Semiconductor detectors gave possibility to measure the radiation power in the frequency range 0.1–0.6 THz. A polychromator with eight frequency selective channels was used for spectral measurements in this frequency range.

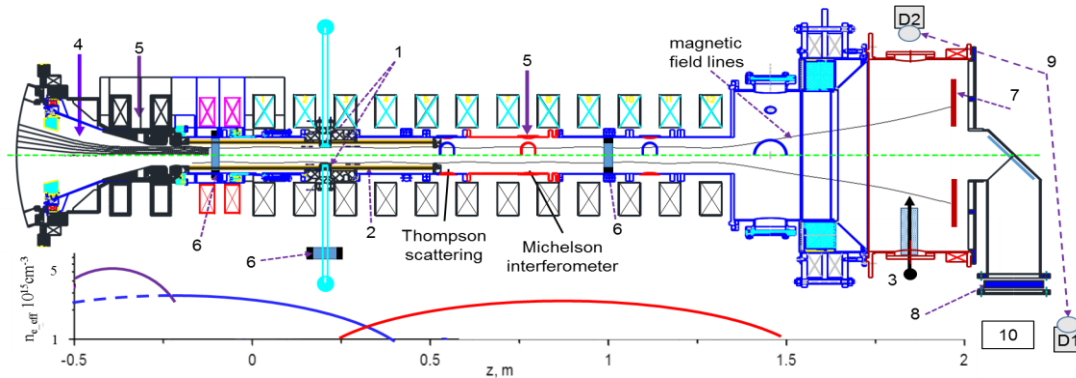


**Figure 1.** Schematic of the GOL-PET facility. 1 discharge electrodes; 2 quartz tube; 3 ignition electrode; 4-5 gas valves; 6 Rogowski coils; 7 beam collector; 8 output window; 9 THz sensors; 10 panel with neon bulbs.

The power density distribution over the cross-section of the flux went out through the output window (8 in Fig. 1) was visualized by the registration of the neon bulbs glow. The bulbs were uniformly distributed over the panel made of a material absorbing the sub-millimeter radiation. Photos of glowing bulbs exposed by the radiation flux were taken with an SDU camera [5].

### Results of experiments

The experiments have shown that for the plasma density  $(0.8 - 1) \cdot 10^{15} \text{ cm}^{-3}$  the main part of THz radiation power propagates along the axis of the plasma column. The spectral power density is concentrated in the region around a frequency of 0.2 THz in which upper-hybrid plasma oscillations exist (see [5]).

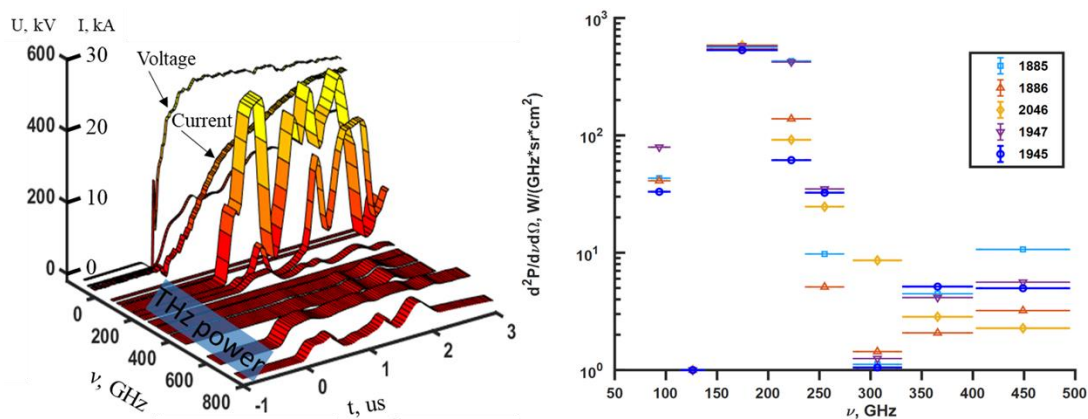


**Figure 2.** The left part shows signal waveforms of the different probes for the shot #1945: U – accelerator diode voltage, I - accelerator diode current, THz power – the radiation power measured in the frequency selective channels of the polychromator (in arb. units). In the right part, spectral composition of the THz radiation flux in case of strong gradients in the plasma density distribution over the diameter of the plasma column.

In the case of replacing the uniform radial distribution of the plasma density with strong gradients in it, the spectral power density of the radiation in the area of the upper-hybrid frequency increased in thirty times. This high-level spectral power density is demonstrated by the spectral composition presented in Fig. 2. This spectrum was measured in 3 meters from the fluoroplastic output window of the vacuum chamber (8 in Fig. 1). The spectral compositions are given for five shots at 1.5  $\mu$ s after beginning of the beam injection. Taking into account the absolute sensitivity of the polychromator channels and the geometry of the experiment setup, we have calculated the power of the radiation flux on the level of 4 MW at the pulse duration up to 4  $\mu$ s.

An additional increase in the radiation flux power by more than 3 times was obtained in the case of a strong decrease in the plasma density in the region near the graphite collector (7 in Fig 1) which absorbs the electron beam. Such flux power gave us the opportunity to visualize the power density distribution over the flux cross section by observing the neon bulbs glow. These distributions for different distances  $L$  from the output window (8 in Fig. 1) are demonstrated by the glow of the neon bulbs shown in the right part of Fig. 3.

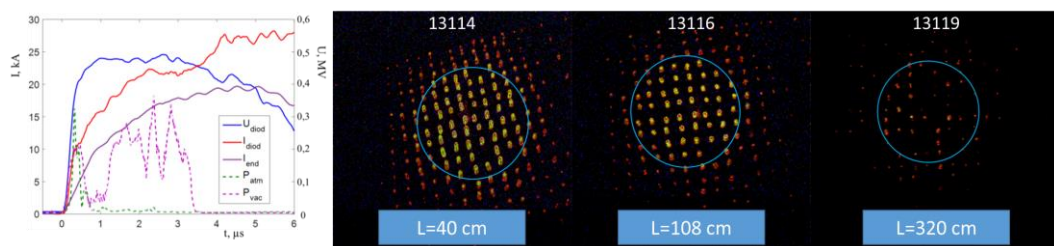


**Figure 3.** The left part shows the waveforms of the voltage on the accelerator diode ( $U_{diode}$ ), the current in the diode ( $I_{diode}$ ) and the beam current at the exit from the plasma column ( $I_{end}$ ). There are the radiation power pulses (arb. units) in the vacuum chamber  $P_{vac}$  and in room atmosphere after passing the output window  $P_{atm}$  also here. The right part demonstrates the glow of the neon bulbs in the panel at different distances  $L$ .

The glowing of the bulbs was occurred as a result of RF breakdown of the neon gas inside their volume. Fig. 3 shows that the radiation flux power is localized in a circular region and is detected after propagation at a distance of 3 m. Nevertheless, the pulse duration of the flux going out from the vacuum chamber through the output window was reduced from 4 to 1  $\mu$ s (see waveforms of the radiation power in Fig.3). We explain this shortening by the development of RF-breakdown on the vacuum side of the output window.

### Discussion of the results

The measurement results of the radiation flux outgoing from the plasma column can be explained in terms of two mechanisms of wave generation in the beam-plasma system. One of them is believed to associate with the linear conversion of superluminal waves driven unstable due to the presence of oblique density modulation  $n = 1 + \Delta n \cos(qr)$ . In such a

plasma, not only Cherenkov beam branch ( $\omega = \omega_p$ ,  $k_{\parallel} = \omega_p/v_b$ ), but also superluminal satellite oscillations ( $\omega = \omega_p$ ,  $k_{\parallel} = \omega_p/v_b - q_{\parallel}$ ) grow with the maximal growth rate. In contrast with the primary unstable wave, the satellite has a magnetic field component and can be linearly converted to EM waves in vacuum. The dispersion curves shown in Fig. 4 demonstrate the principal possibility of this process.

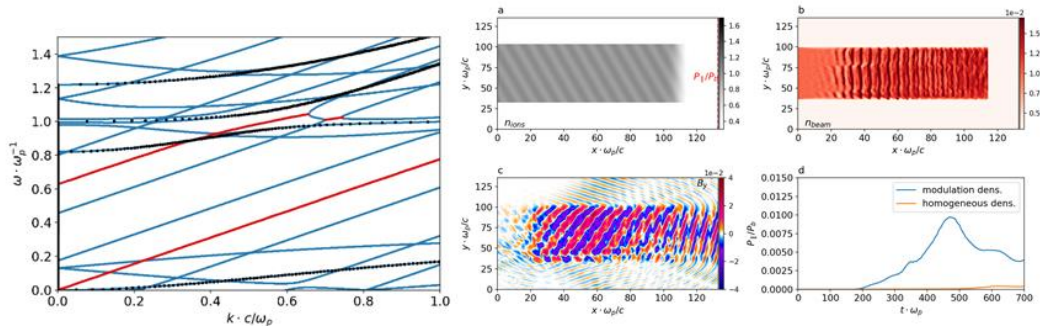


**Figure 4.** In the left part of the figure, the eigen-modes of the system cold relativistic electron beam – cold magnetized plasma with oblique density modulation (red and blue curves correspond to unstable and stable oscillations, respectively, the black curves correspond to the case of the uniform magnetized plasma). In the right part, the results of PIC simulations demonstrating the process of the direct generation of THz radiation by the electron beam: the maps of ion density (a), electron beam density (b), magnetic field (c) and the efficiency of longitudinal beam-to-radiation power conversion as a function of time (d).

Since the typical angular spread of the radiation in experiments is  $\alpha \sim 10^0$ , the transverse wavenumber of density modulation should be estimated as  $q_{\perp} \approx \sin \alpha \sim 0.2 c/\omega_p$ . The highest radiation efficiency is achieved for some specific parallel wavenumbers, for example  $q_{\parallel} = 0.7 c/\omega_p$ , at which another mechanism comes into play and the unstable satellite gets in resonance with stable plasma eigen-modes. This mechanism is clearly observed in PIC simulations (see the right part of Fig. 4). One can see that, in the case of rippled plasma density, the energy transfer from the REB to THz radiation becomes an order of magnitude more efficient compared to the case of homogeneous plasma. According to simulations, about 1% of the beam power can be converted to the power of  $\omega_p$ -radiation propagating at small angles to the plasma column axis.

### Acknowledgment

Part of this work, related to measurements of the spectral composition of the radiation flux was supported by the Russian Science Foundation (project 19-12-00250).

### References

1. A. S. Volokitin and C. Kraff //The Astrophysical Journal Letters, 893:L47 (8pp), 2020 April 20.
2. Arzhannikov A. V. et al 2010 Vestnik Novosibirsk State University. Series: Physics 5, 44
3. Ginzburg V L and Zheleznyakov V V 1958 Sov. Astron. 2 653
4. Benford G, Tzach D, Kato K and Smith D F 1980 Phys. Rev. Lett. 45 1182
5. Arzhannikov A.V., Ivanov I.A., Kasatov A.A., et al. //Plasma physics and controlled fusion. 2020. Vol. 62. № 4. p. 045002. doi.org/10.1088/1361-6587/ab72e3.